This Accepted Manuscript has not been copyedited and formatted. The final version may differ from this version.

Research Articles: Development/Plasticity/Repair

Age-related effects and sex differences in gray matter density, volume, mass, and cortical thickness from childhood to young adulthood

Efstathios D. Gennatas[1], Brian B. Avants[2], Daniel H. Wolf[1], Theodore D. Satterthwaite[1], Kosha Ruparel[1], Rastko Ciric[1], Hakon Hakonarson[3], Raquel E. Gur[1] and Ruben C. Gur[1]

[1]*Brain Behavior Laboratory, Department of Psychiatry, University of Pennsylvania, Philadelphia, PA 19104, USA*
[2]*Penn Image Computing and Science Laboratory, Department of Radiology, University of Pennsylvania, Philadelphia, PA 19104, USA*
[3]*Center for Applied Genomics, Children's Hospital of Philadelphia, Philadelphia, PA 19104, USA*

DOI: 10.1523/JNEUROSCI.3550-16.2017

Received: 17 November 2016

Revised: 21 March 2017

Accepted: 12 April 2017

Published: 21 April 2017

Author contributions: E.D.G. and B.B.A. designed research; E.D.G. performed research; E.D.G., B.B.A., D.H.W., T.D.S., K.R., R.C., H.H., R.E.G., and R.C.G. contributed unpublished reagents/analytic tools; E.D.G. analyzed data; E.D.G., D.H.W., T.D.S., R.E.G., and R.C.G. wrote the paper.

Conflict of Interest: None

This work was supported by NIH grants MH107235, MH089983, MH096891 and the Dowshen Neuroscience fund.

Corresponding author: Efstathios D. Gennatas, Hospital of the University of Pennsylvania, 10 Gates Pavilion, Philadelphia, PA 19104, egenn@upenn.edu

Cite as: J. Neurosci ; 10.1523/JNEUROSCI.3550-16.2017

Alerts: Sign up at www.jneurosci.org/cgi/alerts to receive customized email alerts when the fully formatted version of this article is published.

Accepted manuscripts are peer-reviewed but have not been through the copyediting, formatting, or proofreading process.

Copyright © 2017 the authors

JNeurosci Accepted Manuscript

JNeurosci Accepted Manuscript

Age-related effects and sex differences in gray matter density, volume, mass, and cortical thickness from childhood to young adulthood

Abbreviated Title: Gray matter development in adolescence

Efstathios D. Gennatas[1], Brian B. Avants[2], Daniel H. Wolf[1], Theodore D. Satterthwaite[1], Kosha Ruparel[1], Rastko Ciric[1], Hakon Hakonarson[3], Raquel E. Gur[1], Ruben C. Gur[1]

[1]Brain Behavior Laboratory, Department of Psychiatry, University of Pennsylvania, Philadelphia, PA 19104, USA
[2]Penn Image Computing and Science Laboratory, Department of Radiology, University of Pennsylvania, Philadelphia, PA 19104, USA
[3]Center for Applied Genomics, Children's Hospital of Philadelphia, Philadelphia, PA 19104, USA

Corresponding author
Efstathios D. Gennatas
Hospital of the University of Pennsylvania
10 Gates Pavilion
Philadelphia, PA 19104
egenn@upenn.edu

Number of pages: 27
Number of figures: 5
Number of tables: 4
Multimedia: 1 website
Number of words - Abstract: 197
Introduction: 639
Discussion: 1481

Conflict of Interest: None

Acknowledgements
This work was supported by NIH grants MH107235, MH089983, MH096891 and the Dowshen Neuroscience fund.
We thank PNC participants and their families, as well as the acquisition, assessment, and recruitment team: Monica E. Calkins, Karthik Prabhakaran, Jeffrey Valdez, Marisa Riley, Jack Keefe, Nick DeLeo, Raphael Gerraty, Elliott Yodh, and Rosetta Chiavacci, and Dr. Mark Elliott for contributing the 3D watershed code.
Data deposition: The data reported in this paper has been deposited in the database of Genotypes and Phenotypes (dbGaP; www.ncbi.nlm.nih.gov/gap; Accession No. phs000607.v1.p1).

Keywords
MRI, brain development, brain structure, adolescence, T1-weighted imaging, gray matter density, gray matter volume, gray matter mass, cortical thickness

JNeurosci Accepted Manuscript

ABSTRACT

Developmental structural neuroimaging studies in humans have long described decreases in gray matter volume and cortical thickness during adolescence. Gray matter density, a measure often assumed to be highly related to volume, has not been systematically investigated in development. We used T1 imaging data collected on the Philadelphia Neurodevelopmental Cohort to study age-related effects and sex differences in four regional gray matter measures in 1189 youths aged 8 to 23 years. Custom T1 segmentation and a novel high-resolution gray matter parcellation were used to extract gray matter density (GMD), gray matter volume (GMV), gray matter mass (GMM, defined as GMD * GMV), and cortical thickness (CT) from 1625 brain regions. Non-linear models revealed that each modality exhibits unique age-related effects and sex differences. While GMV and CT generally decrease with age, GMD increases and shows the strongest age-related effects, while GMM shows slight decline overall. Females have lower GMV but higher GMD than males throughout the brain. Our findings suggest that GMD is a prime phenotype for assessment of brain development and likely cognition and that periadolescent gray matter loss may be less pronounced than previously thought. This work highlights the need for combined quantitative histological-MRI studies.

SIGNIFICANCE STATEMENT

This study demonstrates that different MRI-derived gray matter measures show distinct age and sex effects and should not be considered equivalent but complementary. It is shown for the first time that gray matter density increases from childhood to young adulthood, in contrast with gray matter volume and cortical thickness, and that females, known to have lower gray matter volume than males, have higher density throughout the brain. A custom preprocessing pipeline and a novel high-resolution parcellation were created to analyze brain scans of 1189 youths collected as part of the Philadelphia Neurodevelopmental Cohort. A clear understanding of

normal structural brain development is essential for the examination of brain-behavior relationships, the study of brain disease, and, ultimately, clinical applications of neuroimaging.

JNeurosci Accepted Manuscript

JNeurosci Accepted Manuscript

INTRODUCTION

Structural neuroimaging provides insights into the spectrum of typical and non-typical brain and neurocognitive development. T1-weighted imaging is the most commonly acquired MRI sequence and offers high-resolution, low-noise images of brain structure with good tissue contrast. Several structural measures can be derived from a single T1-weighted image, including gray matter density (GMD), gray matter volume (GMV), and cortical thickness (CT). Since the early days of MRI, a large body of research has utilized these measures to study healthy and clinical populations. Perhaps surprisingly, confusion exists in the field as GMD, GMV, and CT are often wrongly assumed to be equivalent or highly related measures of regional gray matter quantity. GMV and CT are measured in mm^3 and mm, respectively. GMD, on the other hand, is a unitless, scalar measure derived from image segmentation and related to T1 signal intensity. In one form or other, gray matter abnormalities have been described in all major neurologic and psychiatric diseases. Voxel Based Morphometry (VBM) analyses have suggested syndrome-specific regional atrophy patterns in neurodegenerative diseases (Seeley et al., 2009). Gray matter abnormalities are widely reported in psychiatric disorders as well but paint a more complex picture (Brent et al., 2013; Bakhshi and Chance, 2015), likely reflecting both increased neuropathological heterogeneity and diagnostic variability. Much of psychopathology emerges around adolescence, a period characterized by rapid changes in behavior. Detecting and interpreting what may often be subtle and diffuse disease-related differences on top of profound and variable age-related changes is particularly challenging. A clear, multidimensional understanding of normative structural brain development is therefore essential.

The first two years of life are characterized by rapid gray matter growth, which reaches its lifetime maximum at around age 2-3 (Matsuzawa et al., 2001; Knickmeyer et al., 2008). In contrast, myelination of white matter tracts continues well into adulthood, until the late 30s (Grydeland et al., 2013). Several developmental neuroimaging studies have described modest

JNeurosci Accepted Manuscript

104 decreases in gray matter during adolescence using measures derived from gray matter volume
105 and cortical thickness (Sowell et al., 2003; Gogtay et al., 2004; Sowell et al., 2004; Shaw et al.,
106 2008; Brain Development Cooperative Group, 2012). It should be noted that some of the early
107 studies used the term “gray matter density” to refer to the proportion of gray matter voxels
108 around a sphere of fixed diameter following hard segmentation of the brain (Sowell et al., 2003;
109 Gogtay et al., 2004; Sowell et al., 2004), and suggested this quantity reflected local cortical
110 thickness. Today, cortical thickness can be measured directly using automated methods and
111 GMD usually refers to a different measure, specifically the output of soft segmentation. Unlike
112 hard segmentation, where each voxel is labeled as “gray”, “white”, or “CSF” (for the common 3-
113 class case), soft segmentation creates a GMD map by assigning voxels a value between zero
114 and one, which is considered to reflect the amount of gray matter in each voxel. It is related to
115 the T1 signal and thus to the regional proton density as well as the tissue microenvironment. To
116 complicate things further, one of the most common measures employed in the literature, and the
117 default option in many VBM pipelines, is “modulated” gray matter density. This is equal to GMD
118 multiplied by a scaling factor to account for volume change from the individual’s native space
119 image to the registration template. It adds to the confusion because the relative contribution of
120 each measure is unclear and likely variable spatially and temporally (with regards to age). To
121 date, no study has compared age-related effects on these four commonly used gray matter
122 measures.

123 In this study, we used the extensive cross-sectional neuroimaging dataset collected on
124 the Philadelphia Neurodevelopmental Cohort (PNC) to characterize age effects and sex
125 differences on native space gray matter density, volume, and mass (defined as density times
126 volume; equivalent to modulated gray matter density), as well as cortical thickness.
127
128 **[FIGURE 1 about here]**
129

JNeurosci Accepted Manuscript

MATERIALS AND METHODS

Subjects and MRI acquisition

All data was collected as part of the Philadelphia Neurodevelopmental Cohort as previously described (Satterthwaite et al., 2014). Procedures were approved by the Institutional Review Boards of the Children's Hospital of Philadelphia and of the University of Pennsylvania. 1189 subjects (648 females) aged 8 to 23 years were selected from a starting total of 1601 after excluding those with neurological or psychiatric history, use of psychoactive medication or incidental findings and those whose structural data failed quality control. Scanning of all subjects was performed on the same Siemens TIM Trio scanner (Erlangen, Germany) at the Hospital of the University of Pennsylvania. T1-weighted imaging was obtained using a magnetization prepared, rapid-acquisition gradient-echo (MPRAGE) sequence (TR = 1810, TE = 3.5, TI = 1100; FOV = 180 RL / 240 AP).

MRI preprocessing

A custom T1 preprocessing pipeline was created using ANTs (https://github.com/stnava/ANTs; RRID: SCR_004757). Raw T1 volumes were first corrected for bias due to field inhomogeneity using the N4 algorithm (Tustison et al., 2010). The bias-corrected volumes were then registered to a whole-head MNI template (whole-head-to-whole-head registration). The inverse transformation was used to map the MNI brain mask to native space, which was used to isolate the brain in native space (skull-stripping). The skull-stripped volume was then registered to the skull-stripped MNI template (brain-to-brain registration), which results in improved registration accuracy compared to the whole-head-to-whole-head registration (Klein et al., 2010). Registrations were performed by a sequence of rigid, affine and symmetric diffeomorphic (SyN) transformations (Avants et al., 2008; Klein et al., 2009).

JNeurosci Accepted Manuscript

Gray matter density and cortical thickness estimation

MRI brain tissue segmentation is commonly guided by a set of tissue priors. Given the wide age range of our sample, we wanted to avoid using a single set of priors for all subjects or different sets of priors for different age bins. We therefore implemented an iterative process based on Atropos (Avants et al., 2011) that requires no tissue priors. On the first iteration, K-means initialization was used to derive 3 classes. The following two iterations used the segmentation output of the previous step for initialization. This procedure resulted in a 3-class hard segmentation and a GMD map (soft segmentation) for each subject in native space (**Figure 1A**). Cortical thickness was obtained using ANTs' diffeomorphic registration-based cortical thickness (DiReCT) estimation procedure (Das et al., 2009) as implemented in the ANTsCT pipeline, following registration of all T1 images to a study-specific template. This method offers reliable CT estimation (Tustison et al., 2014) and, by providing a voxelwise measure in native volumetric space, allows the use of the same brain parcellation as the other modalities.

Quality assurance

To assess the quality of the T1 acquisition and segmentation, we calculated pairwise spatial correlations among all subjects for two sets of images: bias-field corrected, normalized T1s and normalized GMD maps. All images whose spatial correlation was more than two standard deviations lower than the mean in either case were excluded (n = 56). Visual check confirmed variable extent of motion artifact in the excluded images, with those near the threshold being only minimally affected (still excluded). Motion artifact is known to significantly affect tissue segmentation and all our derived measures (Blumenthal et al., 2002; Savalia et al., 2016) and our large sample afforded us this perhaps conservative exclusion threshold.

JNeurosci Accepted Manuscript

High-resolution gray matter parcellation

Multiple methods for whole brain parcellation have been previously proposed. Anatomical parcellations, like the AAL atlas (Tzourio-Mazoyer et al., 2002), and the Harvard-Oxford Atlas (distributed with FSL; https://fsl.fmrib.ox.ac.uk/; RRID:SCR_002823) are based on neuroanatomy but consist of a small number of relatively large regions. Using large parcels or regions of interest (ROIs) runs the risk of averaging over inhomogeneous regions, resulting in signal loss. On the other hand, a number of approaches have been proposed for parcellation based on functional connectivity derived from task-free functional MRI data (also known as resting state fMRI), but none based on T1-weighted images. A recent approach used multimodal MRI data to create a parcellation of 180 regions in each hemisphere. As the authors note, the parcels show high variance in shape and size and consider their number to be "a lower bound, as some parcels are probably complexes of multiple areas" (Glasser et al., 2016).

Our goal was to develop a high-resolution parcellation derived from structural data where parcels are centered around GMD peaks, i.e. cortical gyri and subcortical nuclei. An age- and sex-matched subsample of the 1189 subjects was created by first splitting the initial sample by sex, then splitting each set into deciles based on its age range, and finally randomly selecting 12 subjects from each resulting subset (i.e. 12 subjects per sex per age decile), giving a total of 240 subjects. A mean image was created from the normalized, smoothed GMD maps of these subjects. In order to identify GMD peaks, the gradient of the mean GMD image was calculated, subtracted from 1, and smoothed. A 3D watershed algorithm was applied on the resulting image, producing 1625 parcels covering the whole brain gray matter (**Figure 1B**).

Native space parcelwise data extraction

The GMD1625 parcellation was transformed to each subject's native space by applying the inverse of the brain-to-brain transformation (i.e. MNI-to-native space) and masked by each subject's gray matter hard segmentation. Volume and mean GMD and CT values were

JNeurosci Accepted Manuscript

estimated for each parcel for each subject using the c3d utility (part of ITK-SNAP; http://www.itksnap.org/; RRID: SCR_002010). CT values were measured for 1339 of the 1625 regions, after excluding subcortical regions. In order to get a native space equivalent of modulated density, we derived gray matter mass (GMM) as the product of GMD and GMV. Native space analysis allows direct measurement of GMV and extraction of mean GMD and CT values with no interpolation. Averaging GMD and CT values within each parcel instead of applying Gaussian smoothing avoids smoothing-related artifacts which are exaggerated in a segmented image. Cortical thickness (and therefore the gray matter segmentation) varies around 2-5mm while smoothing kernels are commonly at least 8mm full width at half maximum (FWHM). In a gray matter segmentation, this results in voxel intensities being averaged with surrounding empty voxels (i.e. voxels of zero intensity), causing a drop in signal. The extent of signal drop depends on the number of surrounding empty voxels, which varies both by brain region and age. This makes intensity values from different locations incomparable and directly confounds age-related effects. Interpolation results in a similar artifact, equivalent to smoothing at the single voxel level.

Age-related effects and sex differences

Generalized additive models (GAMs) were used to characterize age-related effects and sex differences on GMD, GMV, GMM, and CT using the mgcv package (Wood, 2011; Wood, 2012) in R (R Project for Statistical Computing; https://www.r-project.org/; RRID:SCR_001905). A GAM is similar to a generalized linear model where predictors can be replaced by smooth functions of themselves, offering efficient and flexible estimation of non-linear effects. Three sets of models were fit. Full models included age and age-by-sex interaction terms represented using penalized smoothing splines with smoothing parameters selected by restricted maximum likelihood. For each modality in turn, for each gray matter parcel *p*, a model of form (1) was fit.

$$\{GMD, GMV, GMM, CT\}_p \sim Sex + s(Age) + s(Age * Sex) \quad (1)$$

JNeurosci Accepted Manuscript

where s() represents a penalized smoothing spline. The dimension of the basis used to represent the smooth terms was limited to a maximum of 5 in all models. Reduced models were fit in order to obtain accurate p-values for the main effects of sex and age. Specifically, model (2) omits the interaction term and was fit for each parcel in order to obtain p-values for the main effect of sex. Model (3) omits sex entirely and was therefore fit separately for each sex *s* in order to obtain p-values for the main effect of age.

$$\{GMD, GMV, GMM, CT\}_p \sim Sex + s(Age) \quad (2)$$

$$\{GMD, GMV, GMM, CT\}_{s,\,p} \sim s(Age) \quad (3)$$

Models of form (3) were also fitted at the whole brain level, using mean GMD and CT (weighted by number of voxels in each parcel), and total GMV and GMM, as separate dependent variables.

$$\{MeanGMD, MeanCT, TotalGMV, TotalGMM\}_{s,\,p} \sim s(Age) \quad (4)$$

In each case, p-values were corrected for multiple comparisons by controlling the false discovery rate (FDR; Benjamini and Hochberg method; q-value = 0.05).

RESULTS

Whole-brain age-related effects: Gray matter density increases while volume and thickness decrease

We sought to characterize age-related effects and sex differences at the whole brain and regional level on three independent gray matter measures, GMD, GMV, and CT, and a derived measure, GMM = GMD * GMV. At the whole brain level, we find that total brain GMV and CT decrease from childhood to young adulthood (8 to 23 years) in accordance with previous studies. In contrast, mean brain GMD increases during the same period. Whole brain GMM shows only a modest decrease. **Figure 2** shows plots of fitted values converted to relative percentages (fitted values for 8 y.o. males are defined as 100%) derived from whole brain

JNeurosci Accepted Manuscript

models (model of form 4 under Materials and Methods, Age-related effects and sex differences). Importantly, GMD is most sensitive to age: 30% and 40% of variance of mean brain GMD is explained by age at scan time for males and females respectively. CT follows with respective values of 30% and 24%, while only 7% and 10% of variance of total brain GMV is explained by age for males and females respectively.

Whole-brain sex differences: Females have lower volume, higher density than males

Females were found to have lower total GMV than males, as expected by known sex differences in average head and brain size. At the same time, however, we show that females have higher mean GMD than males. Total CT was not significantly different between the two sexes in our analysis (**Figure 2**).

[FIGURE 2 about here]

Regional variability in age-related and sex effects

To achieve regional specificity, we created a high-resolution parcellation covering the whole brain gray matter and consisting of 1625 regions. To summarize the large number of regional results, each of the 1625 gray matter parcels was assigned one of nine MNI labels (Frontal Lobe, Temporal Lobe, Parietal Lobe, Occipital Lobe, Insula, Caudate, Putamen, Thalamus, and Cerebellum), as defined by the MNI atlas in FSL. **Table 1** presents summary statistics for each measure aggregated by MNI label. GMM and GMV had the highest coefficient of variation (mean CV = 26.7 and 26.0, respectively), followed by CT (mean CV = 15.6). GMD showed the lowest CV (mean CV = 3.7).

Parcel-wise GAMs were fitted to investigate the regional variability of age-related and sex effects in our sample (1625 parcels for GMD, GMV, and GMM; 1339 for CT). **Table 2** shows the percentage of parcels with significant main effect of age, main effect of sex, and age-by-sex

JNeurosci Accepted Manuscript

interaction after FDR correction (q = 0.05), aggregated by MNI label. GMD showed significant age effects throughout the brain (99% of parcels in males, 99.9% in females), followed by CT (89% males, 88% females). GMV, on the other hand, showed significant age effects only in 52% and 65% of parcels in males and females respectively, while the numbers for GMM were 41% and 33%. Sex effects were strong for GMD, GMV, and GMM. Indeed, main effect of sex was more widespread than main effect of age in GMV and GMM. Sex effects in CT were present in a minority of regions across the whole brain, but in just over half of all temporal and parietal parcels. Age-by-sex interactions were virtually limited to GMD. **Table 3** shows the unadjusted p-value corresponding to FDR q-value of 0.05 and the median of unadjusted p-values surviving FDR correction.

To study the direction of age-related effects in each parcel, the net change from youngest to oldest was estimated by subtracting the fitted value at 8 years from the fitted value at 23 years for each modality, sex, and region and converted to a percentage (by dividing with the fitted values at 8 years). Net change for parcels not surviving FDR correction was set to zero. GMD increased, on average, within all MNI labels, while GMV and CT decreased. Mean GMM decreased in all MNI regions other than the temporal lobe, insula, and cerebellum. The bilateral insula stands out showing the highest increase in GMD and GMM of all MNI regions. To characterize each parcel's sensitivity to age, we examined each model's adjusted R^2, denoting percent variance of each modality's regional values explained by age. **Table 4** lists R^2 and percent change for each modality. Averaging by MNI label masks the variability within each label, for example, a lobe may on average decrease in volume, but some parcels within it may increase. For this reason, **Table 4** includes numbers of individual parcels with a net positive and net negative change from 8 to 23 years within each MNI label. Brain slices mapping net change and R^2 for each modality are shown in **Figure 3** and are available in interactive format online (https://egenn.github.io/gmdvdev.html).

JNeurosci Accepted Manuscript

Figure 4 helps describe how development modulates sex effects by plotting the average difference of male and female fitted values per modality per MNI region by age from 8 to 23 years. Males and females have no differences in GMD at age 8, but females start to lead soon thereafter throughout the brain. Males have higher GMV and GMM on average in each MNI region throughout this age range. Only CT shows a change in the direction of sex differences with age. Males have higher CT in bilateral insula until about age 12 and in frontal and occipital lobes until age 15, at which points the effect reverses leading to a female advantage. In most cases, the sex differences have a nonlinear relationship with age.

[FIGURE 3 about here]

[FIGURE 4 about here]

GMM largely resembles GMV, not GMD

We defined GMM as the product of GMD and GMV in order to study a native-space equivalent of modulated density, a very popular measure in structural neuroimaging studies. GMM showed age-related effects that, for the most part, closely paralleled those of GMV (**Figure 5**). This is probably because GMV has much higher variance than GMD (**Table 1**), and consequently contributes much more to the variance in GMM explained by age than GMD does. Despite this, three MNI regions showed, on average, opposite direction of net change in GMM than in GMV, i.e. an increase instead of a decrease. This was observed in both males and females, in descending order of magnitude, in the insula, the temporal lobe, and the cerebellum (**Table 4**).

Development modulates intermodal relationships among structural measures

To summarize the differences in age-related effects among the four measures with a single quantity, we calculated pairwise correlation coefficients of fitted values for our sample's age range (8 - 23 y.o.; **Figure 5**, top row). Spearman correlation was used as most fitted values are

JNeurosci Accepted Manuscript

non-linear. As expected from the results above, GMD was negatively correlated with GMV and CT throughout the brain and cortex respectively. GMM was positively correlated with GMV and CT in all MNI regions, on average, with the exception of the insula. Looking at the same pairwise correlations among the residuals, i.e. after removing the effect of age, we see that most correlations are positive, with notable exception of the density and thickness pair in the insula (**Figure 5**, bottom row). Intermodal correlations of residuals help suggest what relationships may look like in the absence of an age effect but are no substitute for directly examining separate age bins, which should ideally extend across the lifespan.

[FIGURE 5 about here]

DISCUSSION

Despite extensive use of different MRI-derived gray matter measures in the literature, very few attempts have been made to directly compare them or their developmental patterns, and they are often wrongly assumed to be equivalent. This study shows distinct age-related effects and sex differences on whole brain and regional measures of gray matter density (GMD), volume (GMV), mass (GMM = GMD * GMV), and cortical thickness (CT) in a cross-sectional dataset of 1189 youths aged 8 to 23 years drawn from the Philadelphia Neurodevelopmental Cohort. A custom T1 preprocessing pipeline and a novel high-resolution gray matter parcellation were created in order to produce unbiased gray matter segmentations without use of priors, and to extract native space measures without any interpolation or smoothing. Our findings partly challenge the widely-held, though vague, view that “gray matter declines” from childhood to young adulthood, and provide a more complete description of developmental gray matter differences.

JNeurosci Accepted Manuscript

Not all gray matter declines in adolescence

Mean brain GMD increases from childhood to young adulthood, while total brain GMV and mean CT decrease. Total GMM only shows a slight decrease from 8 to 23 years, suggesting that an increase in density may partly counter a decrease in volume. Regionally, GMD increases virtually throughout the brain. GMV, on the other hand, decreases on average in all lobes and subcortical regions, but there are parcels within those broad regions whose volume increases, particularly in frontotemporal cortex. Future work will determine whether areas that expand during adolescence despite an overall decline in volume support the enhancement of specific neurocognitive functions.

Age-related effects and sex differences in density may help understand cognitive abilities

We know that higher GMV correlates with higher neurocognitive performance in adults (Gur et al., 1999; McDaniel, 2005), which gives rise to two apparent paradoxes: 1. Adolescence is characterized by a sharp rise in neurocognitive performance (Gur and Gur, 2016), despite a decline in GMV. 2. There are no significant sex differences in general intelligence (Halpern et al., 2007), despite a male advantage in GMV. Our results suggest that age-associated volume decrease might be compensated for by increasing gray matter density during adolescence and lower volume in females might be compensated for by higher density throughout the brain.

Biological basis of structural MR measures: the need for large scale, quantitative histological – MRI studies

The above findings beg the question: What do GMD and the other gray matter measures mean in terms of biology? Multiple studies have shown that the T1 signal is sensitive to myelin and iron content, whose distributions overlap significantly within cortical gray matter (Stüber et al., 2014). Surprisingly, only few attempts have been made to quantify the relationships among

JNeurosci Accepted Manuscript

386 histological features and MRI-derived structural measures. A large number of studies using T1-
387 weighted imaging to quantify gray matter have focused on neurodegeneration. Such diseases
388 result in neuronal loss which causes direct decreases in all gray matter measures. This may
389 partly explain the confusion that has led to these measures often being considered highly
390 correlated or equivalent, and even grouped together in meta-analyses (for example, see Shao
391 et al., 2014). However, in the context of normal brain structure, or in brain disease without
392 extensive neuronal loss, including most psychiatric disorders, regional and global variation in
393 different gray matter measures may be less correlated, even anti-correlated, as seen here
394 between GMD and GMV. We expect that MRI-derived gray matter measures are differentially
395 determined by a set of histological factors, including neuronal and glial number and size,
396 dendritic arborization, number of axonal projections and extent of myelination. Their effects will
397 vary by age, brain region, and cortical layer.

398 In adolescence, MRI-estimated decline in gray matter volume is generally attributed to a
399 combination of synaptic pruning of exuberant connections, a regressive event, and increasing
400 myelination, a progressive event, both essential aspects of normal development (Stiles and
401 Jernigan, 2010). While pruning results in a direct reduction in neuropil, myelination may have
402 multiple direct and indirect effects on T1-based gray matter quantification. White matter
403 myelination and expansion may result in a physical outwards shift of the gray-white matter
404 boundary causing gray matter to compact and leading to decreases in GMV and CT and
405 increases in GMD. Alternatively, myelination near the gray-white border may increase signal
406 intensity in voxels nearest the border enough to switch their classification from gray to white,
407 which would lead to reduction of volume and thickness measurements but have no effect on
408 density, since these voxels would be now excluded from any gray matter parcels. At the same
409 time, cortical gray matter also contains substantial amounts of myelinated fibers with significant
410 regional variability (Nieuwenhuys, 2013) and intracortical myelin also increases during
411 adolescence (Grydeland et al., 2013). Increasing cortical myelination would lead to a decrease

JNeurosci Accepted Manuscript

412 in estimated GMD, which means that GMD increases reported in this study are possibly
413 underestimates. Rabinowicz et al performed stereologic morphometry in six males and five
414 females aged 12 to 24 years and reported significantly higher neuronal densities and neuronal
415 number estimates in males than females, but no sex differences in cortical thickness,
416 suggesting higher neuropil mass / increased neuronal processes in the female cortex
417 (Rabinowicz et al., 2009), which might explain our findings of higher GMD in females.
418 We chose to compare four different measures of regional gray matter in volumetric
419 space. Other morphometric and morphological measures like cortical surface area and
420 gyrification index can also be derived from T1 images in surface space analyses. The limited
421 positive correlation we found between GMV and CT age-related effects is probably explained by
422 independent changes in surface area and gyrification (Raznahan et al., 2011). While the
423 majority of brain regions show significant sex effects on GMV as expected, a minority of regions
424 showed a significant sex effect on CT. Considering that gray matter volume roughly equals
425 surface area times cortical thickness, we expect surface area to exhibit more extensive sex
426 differences than thickness. We limited our analysis to volumetric space measures in order to
427 use the same parcellation for each measure and avoid the extra resampling and registration
428 errors introduced in the conversion between the two spaces (Klein et al., 2010). For the same
429 reason, care must be taken when comparing volumetric and surface space analyses.
430 Given the important gaps in our understanding of the links between biology and imaging,
431 it is crucial to design large-scale, combined MRI and histological quantification studies to fully
432 characterize the neurobiological basis of raw MRI signals and derived measures. Biophysical
433 modeling of MR-derived measures will enable accurate noninvasive in vivo prediction of
434 histological features (Stiles and Jernigan, 2010). This will be crucial in elevating the potential of
435 neuroimaging in the investigation of nervous system physiology and pathology, disease
436 diagnosis, and treatment monitoring.
437

JNeurosci Accepted Manuscript

Limitations and implication for future work: Phenotypes of structural brain development and links to cognition

The cross-sectional design of this study was its main limitation. Ongoing longitudinal studies will provide true measures of developmental change and allow the analysis of inter-individual differences in development. Future studies would also benefit from inclusion of more MRI modalities. New diffusion-weighted MRI techniques like neurite orientation dispersion and density imaging (NODDI) may provide rich information on gray matter structure and complement T1 and T2 signals (Zhang et al., 2012). Histological morphometry has shown cortical layer- and type-specific changes in neuronal cell bodies (Rabinowicz et al., 2009), which cannot be resolved with today's common MRI sequences but this may be possible in the future. We must note that while different segmentation software employ similar methods for GMD estimation, results are dependent on parameter selection. Correlation with histology will also help guide these choices and optimize pipelines to produce measures with maximal biological interpretability.

Our results demonstrate that GMD, GMV, and CT must be considered distinct and complementary. They also further emphasize the need for nonlinear modeling and accounting for sex differences. We found that GMD and CT are most sensitive to age, which makes them prime candidate biomarkers of brain development. In contrast, modulated density or GMM may not be very informative in a developmental context, and it is best to consider GMD and GMV independently. We also show that intermodal relationships change with age, which further emphasizes that neuroimaging findings should not be generalized from one age period to another. We have previously shown that structural covariance networks develop during childhood to mirror adult functional intrinsic connectivity networks (Zielinski et al., 2010). Ongoing work aims to identify how different structural measures can be best applied to study cognition and disease.

JNeurosci Accepted Manuscript

As we advance from group-level to individual-level studies, from unimodal to multimodal analyses, and from descriptive to predictive models with the aim of integrating neuroimaging into clinical practice, it is essential to make best use of all available data. The first step is to understand available measures and the relationships among them. Development is a critical dimension on which these relationships may vary and adds to the challenge and the importance of this task.

JNeurosci Accepted Manuscript

472 **REFERENCES**

473 Avants BB, Epstein CL, Grossman M, Gee JC (2008) Symmetric diffeomorphic image
474 registration with cross-correlation: evaluating automated labeling of elderly and
475 neurodegenerative brain. Med Image Anal 12:26–41.

476 Avants BB, Tustison NJ, Wu J, Cook PA, Gee JC (2011) An open source multivariate
477 framework for n-tissue segmentation with evaluation on public data.
478 Neuroinformatics 9:381–400.

479 Bakhshi K, Chance SA (2015) The neuropathology of schizophrenia: A selective review
480 of past studies and emerging themes in brain structure and cytoarchitecture.
481 Neuroscience 303:82–102.

482 Blumenthal JD, Zijdenbos A, Molloy E, Giedd JN (2002) Motion artifact in magnetic
483 resonance imaging: implications for automated analysis. Neuroimage 16:89–92.

484 Brain Development Cooperative Group (2012) Total and regional brain volumes in a
485 population-based normative sample from 4 to 18 years: the NIH MRI Study of
486 Normal Brain Development. Cerebral Cortex 22:1–12.

487 Brent BK, Thermenos HW, Keshavan MS, Seidman LJ (2013) Gray matter alterations in
488 schizophrenia high-risk youth and early-onset schizophrenia: a review of structural
489 MRI findings. Child Adolesc Psychiatr Clin N Am 22:689–714.

490 Das SR, Avants BB, Grossman M, Gee JC (2009) Registration based cortical thickness
491 measurement. 45:867–879.

492 Glasser MF, Coalson TS, Robinson EC, Hacker CD, Harwell J, Yacoub E, Ugurbil K,

JNeurosci Accepted Manuscript

493 Andersson J, Beckmann CF, Jenkinson M, Smith SM, Van Essen DC (2016) A
494 multi-modal parcellation of human cerebral cortex. Nature 536:171–178.

495 Gogtay N, Giedd JN, Lusk L, Hayashi KM, Greenstein D, Vaituzis AC, Nugent TF,
496 Herman DH, Clasen LS, Toga AW, Rapoport JL, Thompson PM (2004) Dynamic
497 mapping of human cortical development during childhood through early adulthood.
498 Proc Natl Acad Sci USA 101:8174–8179.

499 Grydeland H, Walhovd KB, Tamnes CK, Westlye LT, Fjell AM (2013) Intracortical
500 myelin links with performance variability across the human lifespan: results from T1-
501 and T2-weighted MRI myelin mapping and diffusion tensor imaging. J Neurosci
502 33:18618–18630.

503 Gur RC, Turetsky BI, Matsui M, Yan M, Bilker W, Hughett P, Gur RE (1999) Sex
504 differences in brain gray and white matter in healthy young adults: correlations with
505 cognitive performance. 19:4065–4072.

506 Gur RE, Gur RC (2016) Sex differences in brain and behavior in adolescence: Findings
507 from the Philadelphia Neurodevelopmental Cohort. Neurosci Biobehav Rev.

508 Halpern DF, Benbow CP, Geary DC, Gur RC, Hyde JS, Gernsbacher MA (2007) The
509 Science of Sex Differences in Science and Mathematics. Psychol Sci Public Interest
510 8:1–51.

511 Klein A, Andersson J, Ardekani BA, Ashburner J, Avants B, Chiang M-C, Christensen
512 GE, Collins DL, Gee J, Hellier P, Song JH, Jenkinson M, Lepage C, Rueckert D,
513 Thompson P, Vercauteren T, Woods RP, Mann JJ, Parsey RV (2009) Evaluation of

JNeurosci Accepted Manuscript

14 nonlinear deformation algorithms applied to human brain MRI registration. 46:786–802.

Klein A, Ghosh SS, Avants B, Yeo BTT, Fischl B, Ardekani B, Gee JC, Mann JJ, Parsey RV (2010) Evaluation of volume-based and surface-based brain image registration methods. Neuroimage 51:214–220.

Knickmeyer RC, Gouttard S, Kang C, Evans D, Wilber K, Smith JK, Hamer RM, Lin W, Gerig G, Gilmore JH (2008) A structural MRI study of human brain development from birth to 2 years. 28:12176–12182.

Matsuzawa J, Matsui M, Konishi T, Noguchi K, Gur RC, Bilker W, Miyawaki T (2001) Age-related volumetric changes of brain gray and white matter in healthy infants and children. Cereb Cortex 11:335–342.

MCDANIEL M (2005) Big-brained people are smarter: A meta-analysis of the relationship between in vivo brain volume and intelligence. Intelligence 33:337–346.

Nieuwenhuys R (2013) The myeloarchitectonic studies on the human cerebral cortex of the Vogt-Vogt school, and their significance for the interpretation of functional neuroimaging data. Brain structure & function 218:303–352.

Rabinowicz T, Petetot JM-C, Khoury JC, de Courten-Myers GM (2009) Neocortical maturation during adolescence: change in neuronal soma dimension. Brain Cogn 69:328–336.

Raznahan A, Shaw P, Lalonde F, Stockman M, Wallace GL, Greenstein D, Clasen L, Gogtay N, Giedd JN (2011) How does your cortex grow? 31:7174–7177.

JNeurosci Accepted Manuscript

535 Savalia NK, Agres PF, Chan MY, Feczko EJ, Kennedy KM, Wig GS (2016) Motion-
536 related artifacts in structural brain images revealed with independent estimates of in-
537 scanner head motion. Human brain mapping.

538 Seeley WW, Crawford RK, Zhou J, Miller BL, Greicius MD (2009) Neurodegenerative
539 diseases target large-scale human brain networks. Neuron 62:42–52.

540 Shao N, Yang J, Li J, Shang H-F (2014) Voxelwise meta-analysis of gray matter
541 anomalies in progressive supranuclear palsy and Parkinson's disease using
542 anatomic likelihood estimation. Front Hum Neurosci 8:63.

543 Shaw P, Kabani NJ, Lerch JP, Eckstrand K, Lenroot R, Gogtay N, Greenstein D, Clasen
544 L, Evans A, Rapoport JL, Giedd JN, Wise SP (2008) Neurodevelopmental
545 trajectories of the human cerebral cortex. 28:3586–3594.

546 Sowell ER, Peterson BS, Thompson PM, Welcome SE, Henkenius AL, Toga AW (2003)
547 Mapping cortical change across the human life span. Nat Neurosci 6:309–315.

548 Sowell ER, Thompson PM, Toga AW (2004) Mapping changes in the human cortex
549 throughout the span of life. The Neuroscientist 10:372–392.

550 Stiles J, Jernigan TL (2010) The basics of brain development. Neuropsychol Rev
551 20:327–348.

552 Stüber C, Morawski M, Schäfer A, Labadie C, Wähnert M, Leuze C, Streicher M,
553 Barapatre N, Reimann K, Geyer S, Spemann D, Turner R (2014) Myelin and iron
554 concentration in the human brain: A quantitative study of MRI contrast. Neuroimage
555 93:95–106.

JNeurosci Accepted Manuscript

556 Tustison NJ, Avants BB, Cook PA, Zheng Y, Egan A, Yushkevich PA, Gee JC (2010)
557 N4ITK: improved N3 bias correction. IEEE Trans Med Imaging 29:1310–1320.

558 Tustison NJ, Cook PA, Klein A, Song G, Das SR, Duda JT, Kandel BM, van Strien N,
559 Stone JR, Gee JC, Avants BB (2014) Large-scale evaluation of ANTs and
560 FreeSurfer cortical thickness measurements. 99:166–179.

561 Tzourio-Mazoyer N, Landeau B, Papathanassiou D, Crivello F, Etard O, Delcroix N,
562 Mazoyer B, Joliot M (2002) Automated anatomical labeling of activations in SPM
563 using a macroscopic anatomical parcellation of the MNI MRI single-subject brain.
564 15:273–289.

565 Wood SN (2011) Fast stable restricted maximum likelihood and marginal likelihood
566 estimation of semiparametric generalized linear models. J R Stat Soc Series B Stat
567 Methodol 73:3–36.

568 Wood SN (2012) On p-values for smooth components of an extended generalized
569 additive model. Biometrika:ass048.

570 Zhang H, Schneider T, Wheeler-Kingshott CA, Alexander DC (2012) NODDI: practical
571 in vivo neurite orientation dispersion and density imaging of the human brain.
572 Neuroimage 61:1000–1016.

573 Zielinski BA, Gennatas ED, Zhou J, Seeley WW (2010) Network-level structural
574 covariance in the developing brain. Proc Natl Acad Sci USA 107:18191–18196.

575

576

JNeurosci Accepted Manuscript

FIGURE LEGENDS

Figure 1. T1 preprocessing and high-resolution gray matter parcellation

(A) Raw T1 MPRAGE volumes were first corrected for field inhomogeneity and then skull-stripped by transforming the MNI brain mask to native space. Gray matter segmentation was performed without the use of tissue priors to produce unbiased estimates of gray matter density (GMD).

(B) The GMD maps of an age- and sex-balanced subsample of 240 subjects were averaged and smoothed. 1 minus the gradient of the resulting image was calculated and passed to a 3D watershed algorithm, resulting in 1625 regions covering the whole brain gray matter.

Figure 2. Density increases in adolescence while other measures largely decrease. Females have higher density, lower volume.

Plots show fitted values of whole brain gray matter measures against age for the two sexes. GMD and CT were averaged across the brain (weighted by N of voxels in each parcel), GMV and GMM were summed. To make results comparable across measures, they are plotted as percentages. 100% is defined as the fitted value for males at 8 years. Shaded bands correspond to ± 2 * standard error of the fit (~95% confidence interval).

Figure 3. Percent net change and variance explained by sex and modality

(A) For each parcel, percent net change was calculated as:

(fitted value at 23 – fitted value at 8) / (fitted value at 8) * 100%

GMD increased virtually throughout the brain, while the other modalities show mostly decreases. Females showed greater increase in density than males throughout the brain.

(B) Percent variance of each measure explained by age. GMD showed the highest R^2 values, followed by CT.

High bilateral symmetry on all maps suggests biological plausibility.

JNeurosci Accepted Manuscript

Interactive movies including all axial slices in this figure are available online at https://egenn.github.io/gmdvdev

Figure 4. Sex differences by modality by MNI region against age

The difference of male and female fitted values for each modality for each MNI region was calculated at each year from 8 to 23. This plot highlights qualitatively how sex differences vary with age, in most cases in a non-linear fashion (a constant sex difference in any measure would appear as a horizontal line). Note that only in CT the direction of the difference changes in frontal and occipital lobes as well as the bilateral insula from a male to a female advantage.

Figure 5. Intermodal correlations averaged by MNI label

Pairwise spearman correlations were estimated between the fitted values of model (3) (top row) of all gray matter measures in order to summarize the similarity of age-related effects among modalities and between their residuals (bottom row). Brain slices with these results are available online at https://egenn.github.io/gmdvdev/imcor.html

D: gray matter density; **V:** gray matter volume; **M:** gray matter mass; **T:** cortical thickness.

JNeurosci Accepted Manuscript

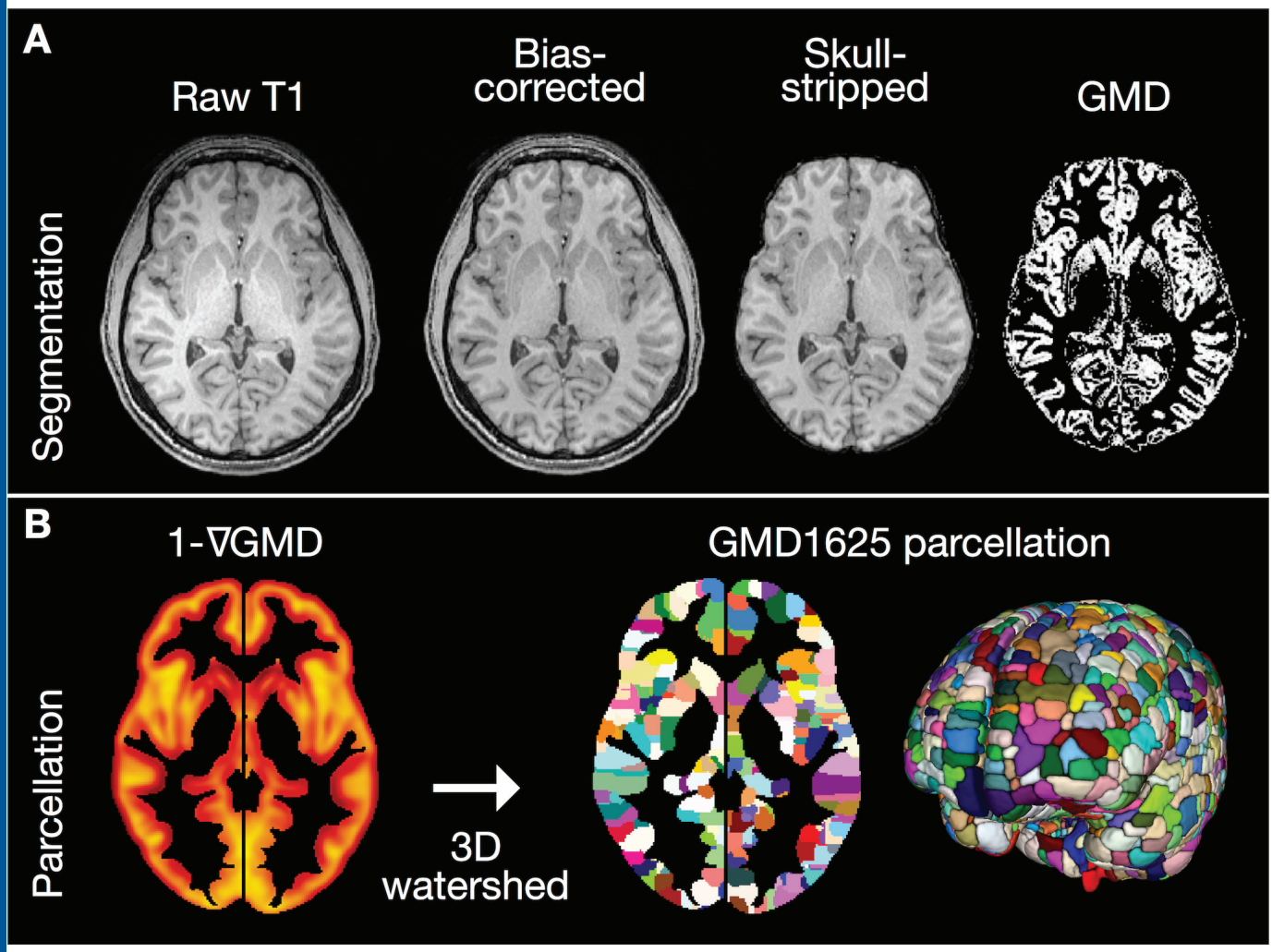

JNeurosci Accepted Manuscript

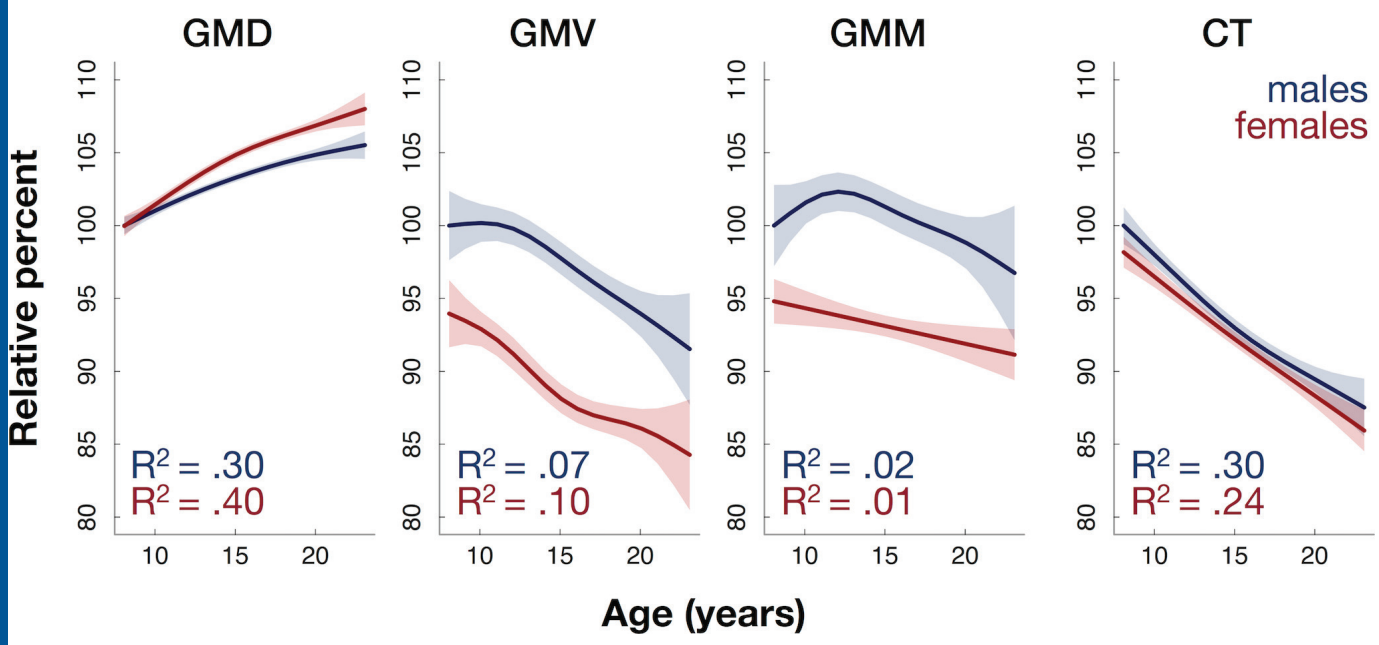

JNeurosci Accepted Manuscript

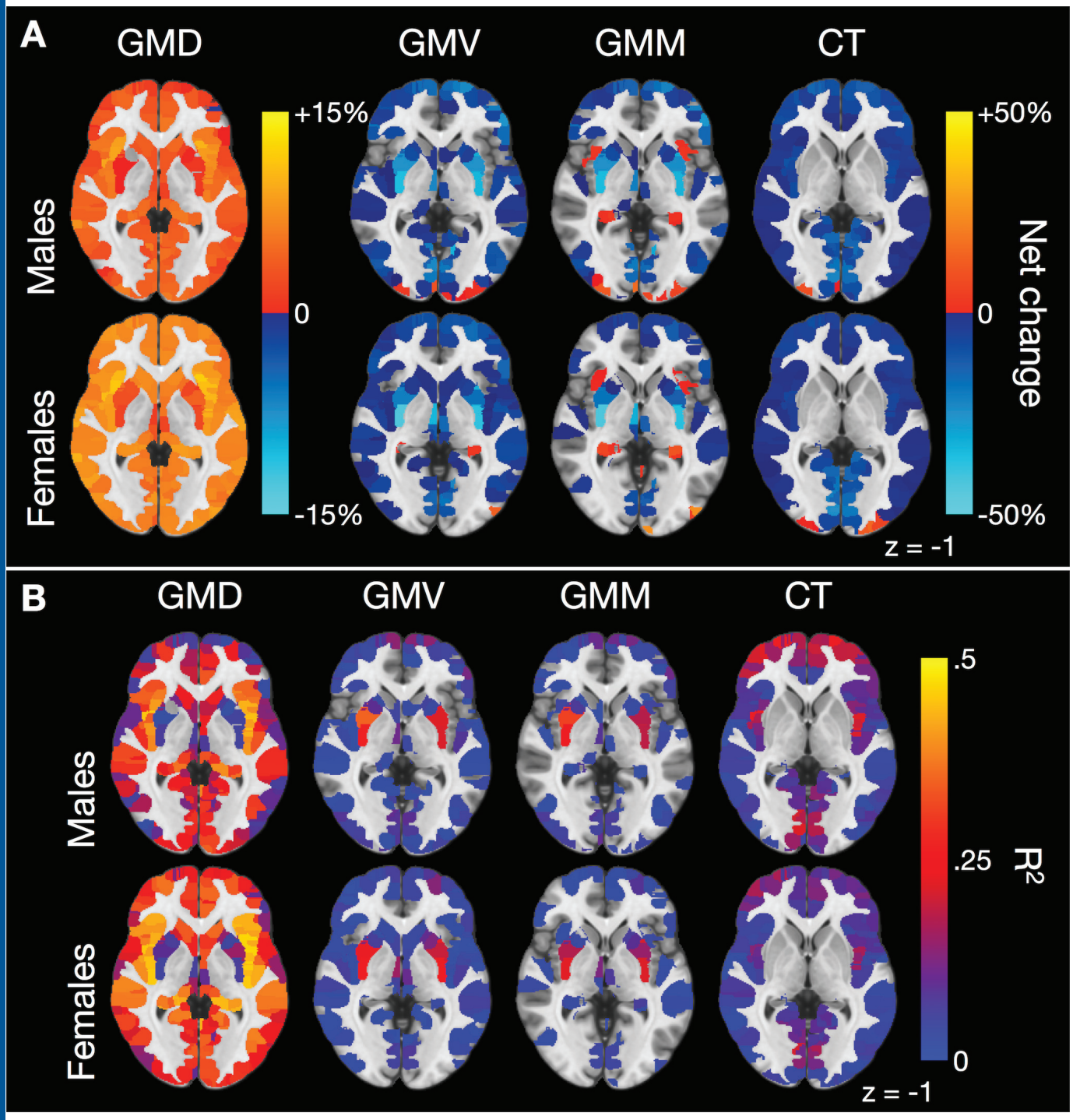

JNeurosci Accepted Manuscript

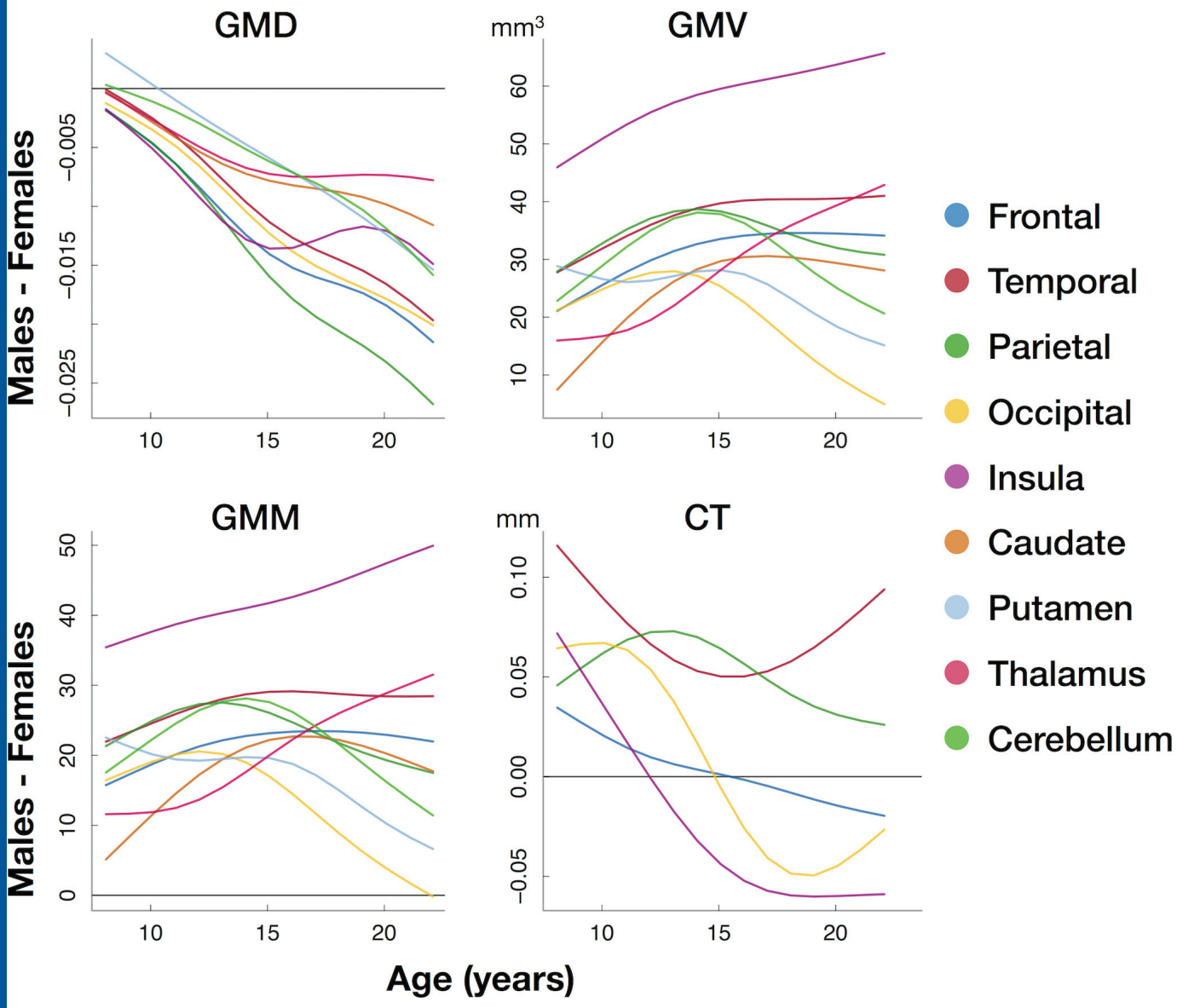

JNeurosci Accepted Manuscript

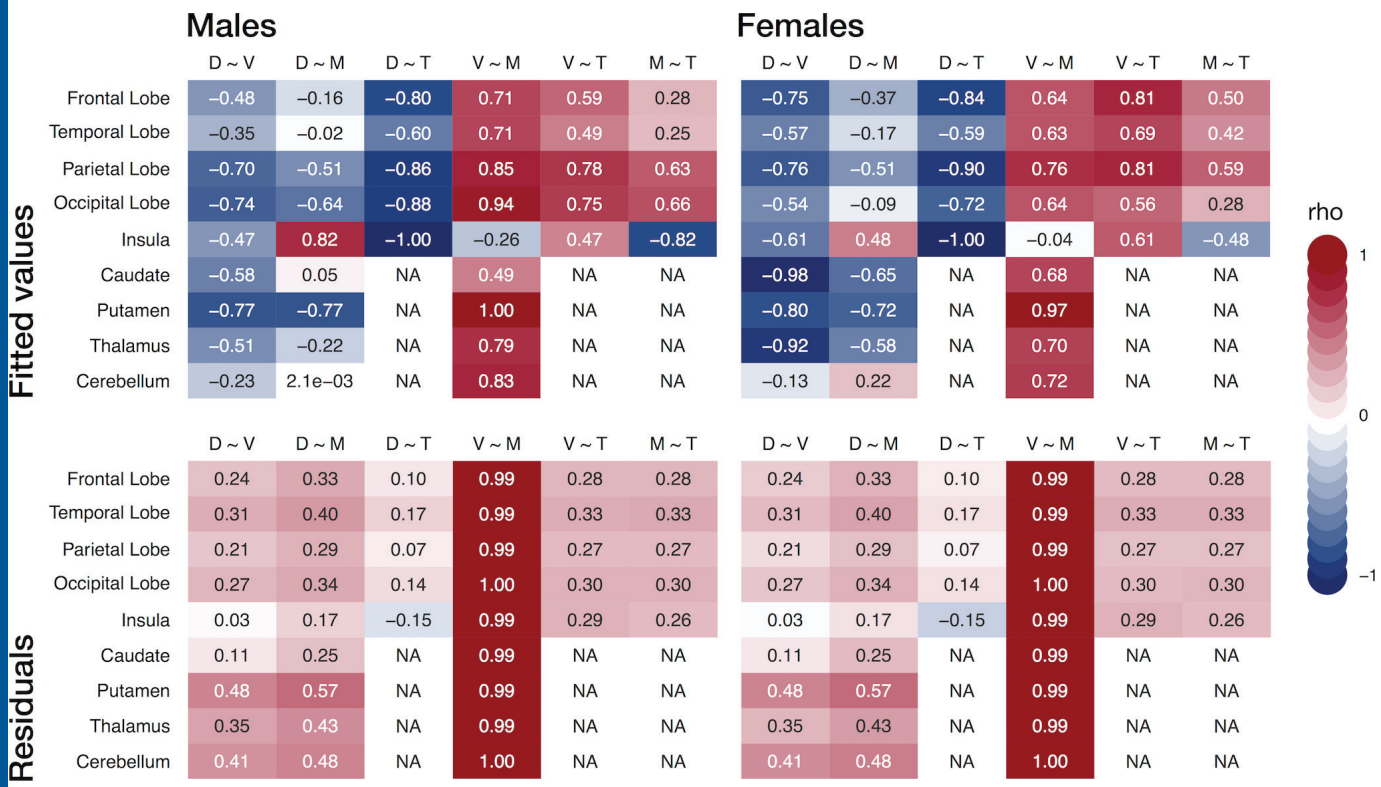

JNeurosci Accepted Manuscript

Summary statistics of regional gray matter measures averaged by MNI label

	GMD			GMV			GMM			CT			N total
MNI label	**Mean**	**SD**	**CV**	**Mean**	**SD**	**CV**	**Mean**	**SD**	**CV**	**Mean**	**SD**	**CV**	
Frontal	0.82	0.03	3.96	359.75	99.73	27.72	295.18	83.19	28.18	3.57	0.53	14.82	514
Temporal	0.82	0.03	3.77	352.64	94.07	26.68	290.09	79.32	27.34	4.03	0.60	14.86	319
Parietal	0.82	0.03	3.79	385.09	114.59	29.76	317.25	95.28	30.03	3.34	0.53	15.88	294
Occipital	0.80	0.03	3.54	290.55	95.01	32.70	235.55	78.16	33.18	3.27	0.62	18.86	190
Insula	0.83	0.03	3.76	578.78	106.87	18.47	478.39	88.37	18.47	4.53	0.61	13.49	22
Caudate	0.84	0.03	3.20	374.18	61.72	16.50	313.19	52.72	16.83	-	-	-	25
Putamen	0.76	0.03	4.12	317.26	92.32	29.10	242.50	74.38	30.67	-	-	-	23
Thalamus	0.77	0.03	3.38	316.30	80.05	25.31	246.39	64.68	26.25	-	-	-	25
Cerebellum	0.80	0.03	3.74	340.28	94.78	27.85	273.04	78.83	28.87	-	-	-	213

Table 1. SD: Standard deviation, **CV:** Coefficient of variation (a.k.a. relative standard deviation). **N total:** Total number of parcels within MNI label (out of 1625)

JNeurosci Accepted Manuscript

Generalized Additive Models: Main effects and interaction by MNI label

MNI label	Main effect of age								Main effect of sex				Age by sex interaction				N total
	GMD		GMV		GMM		CT										
	M	F	M	F	M	F	M	F	GMD	GMV	GMM	CT	GMD	GMV	GMM	CT	
Frontal	99	100	44	67	35	27	92	91	100	88	81	24	79	4	7	1	514
Temporal	100	100	43	65	35	34	75	78	99	95	91	56	94	2	2	1	319
Parietal	98	100	64	74	46	38	96	93	99	84	80	52	91	4	6	4	294
Occipital	99	100	69	47	49	18	92	84	96	74	78	44	92	8	16	15	190
Insula	100	100	14	59	32	32	100	100	100	100	100	14	45	0	0	0	22
Caudate	96	100	24	92	20	32	-	-	100	96	96	-	44	4	4	-	25
Putamen	83	91	100	100	100	96	-	-	70	91	87	-	61	9	13	-	23
Thalamus	100	100	64	76	48	64	-	-	88	96	96	-	32	8	8	-	25
Cerebellum	100	100	51	54	48	46	-	-	79	87	85	-	66	2	4	-	213

Table 2A. Percent of parcels with significant effects after FDR correction for multiple comparisons

JNeurosci Accepted Manuscript

Generalized Additive Models: FDR Threshold and median p-values

			Threshold	Median
Main effect of age	GMD	M	0.0494	2.005E-24
		F	0.0500	3.096E-47
	GMV	M	0.0276	2.359E-04
		F	0.0337	2.516E-04
	GMM	M	0.0227	2.612E-04
		F	0.0197	2.516E-04
	CT	M	0.0448	2.195E-09
		F	0.0442	2.989E-10
Main effect of sex	GMD		0.0480	1.437E-12
	GMV		0.0446	1.448E-09
	GMM		0.0427	9.395E-08
	CT		0.0231	5.327E-04
Age by sex interaction	GMD		0.0414	6.223E-04
	GMV		0.0029	3.427E-04
	GMM		0.0038	6.872E-04
	CT		0.0032	6.512E-05

Table 3. Threshold: Unadjusted p-value corresponding to FDR q-value = 0.05
Median: Median of unadjusted p-values surviving FDR correction

JNeurosci Accepted Manuscript

Net percent change from 8 to 23 years and variance explained by MNI label

MALES

	GMD				GMV				GMM				CT				
MNI label	**R^2**	**Pct**	**N ↑**	**N ↓**	**R^2**	**Pct**	**N ↑**	**N ↓**	**R^2**	**Pct**	**N ↑**	**N ↓**	**R^2**	**Pct**	**N ↑**	**N ↓**	**N total**
Frontal	0.181	5.48	507	1	0.015	-5.34	35	193	0.012	-1.37	66	116	0.088	-12.75	23	450	514
Temporal	0.207	5.79	319	0	0.013	-2.69	45	92	0.015	1.70	69	44	0.027	-5.43	30	209	319
Parietal	0.168	4.99	288	0	0.021	-10.17	12	176	0.015	-5.22	24	112	0.097	-15.87	4	278	294
Occipital	0.170	5.09	189	0	0.026	-11.02	13	118	0.018	-6.33	15	78	0.063	-14.11	5	169	190
Insula	0.393	8.51	22	0	0.002	-1.04	0	3	0.008	3.63	7	0	0.140	-17.49	0	22	22
Caudate	0.202	4.78	24	0	0.009	-3.15	0	6	0.006	-0.27	3	2		-	-	-	25
Putamen	0.058	2.60	18	1	0.122	-28.70	0	23	0.097	-26.76	0	23		-	-	-	23
Thalamus	0.222	5.59	25	0	0.034	-10.60	2	14	0.028	-5.92	3	9		-	-	-	25
Cerebellum	0.216	5.78	213	0	0.028	-3.02	32	76	0.025	0.91	50	53		-	-	-	213

FEMALES

	GMD				GMV				GMM				CT				
MNI label	**R^2**	**Pct**	**N ↑**	**N ↓**	**R^2**	**Pct**	**N ↑**	**N ↓**	**R^2**	**Pct**	**N ↑**	**N ↓**	**R^2**	**Pct**	**N ↑**	**N ↓**	**N total**
Frontal	0.263	8.21	514	0	0.017	-8.68	22	321	0.007	-0.84	40	100	0.075	-11.15	25	444	514
Temporal	0.296	8.51	319	0	0.016	-6.48	40	167	0.013	1.89	60	47	0.026	-5.27	36	214	319
Parietal	0.293	8.41	294	0	0.022	-12.16	6	213	0.009	-3.36	20	93	0.092	-14.86	8	266	294
Occipital	0.262	7.66	190	0	0.012	-6.65	5	85	0.004	-1.48	7	27	0.045	-10.81	15	146	190
Insula	0.430	10.39	22	0	0.010	-5.42	0	13	0.006	2.92	7	0	0.095	-15.16	0	22	22
Caudate	0.243	6.36	25	0	0.032	-10.65	0	23	0.006	-2.97	0	8		-	-	-	25
Putamen	0.107	5.24	21	0	0.125	-26.15	0	23	0.091	-21.99	0	22		-	-	-	23
Thalamus	0.256	6.61	25	0	0.067	-19.71	0	19	0.046	-14.91	2	14		-	-	-	25
Cerebellum	0.259	8.16	213	0	0.021	-3.70	26	88	0.016	2.18	49	48		-	-	-	213

Table 4. Pct: Percent change of fitted values from 8 to 23 years. **N ↑:** Number of parcels with positive net change (increase); **N ↓**: Number of parcels with negative net change (decrease).
Only parcels that survived FDR correction have been considered.